

# Hybrid Acquisition of CBOC Galileo Signals under Multiple Correct-window Hypothesis

Elena Simona Lohan

Department of Communications Engineering  
Tampere University of Technology (TUT Foundation)  
Tampere, Finland  
elena-simona.lohan[at]tut[dot]fi

Alexandru Rusu Casandra and Ion Marghescu

Faculty of Electronics, Telecommunications and  
Information Technology  
University Politehnica of Bucharest  
Bucharest, Romania  
rusu.alex[at]yahoo[dot]com, marion[at]comm.pub.ro

**Abstract**— This paper computes the mean acquisition time for a hybrid search acquisition stage of Galileo signals, under the assumption of multiple correct windows in the search space. The assumption of multiple correct windows is a realistic assumption both in single and multipath-fading channels, due to the fact that the width of the main lobe of the correlation envelope is at least 2 chips (depending on the receiver front-end bandwidth) and the time-bin step of scanning the multiple code phases is typically below 0.5 chips. The multiple-window hypothesis acquisition is poorly addressed in the Code Division Multiple Access (CDMA) literature, and the comparison of multiple-dwell acquisition strategy is completely novel in the Global Navigation Satellite System (GNSS) literature, to the best of the authors' knowledge. One of the main results of the paper is that choosing an increased false alarm probability per dwell when going from one dwell to the next one, in conjunction with an increasing integration time, offers better results for the mean acquisition time.

**Keywords**—unambiguous code acquisition, Galileo, hybrid search, multiple correct-window hypothesis

## I. BACKGROUND AND PROBLEM DEFINITION

In 1998, the European Union decided to pursue a satellite navigation system independent of the U.S. Global Positioning System. This European satellite system, namely Galileo, is designed specifically for civilian use worldwide. When completed, the Galileo system will provide multiple levels of service to users throughout the world. This paper studies the acquisition of Galileo E1 Open Service (OS) signals with multi-dwell hybrid search acquisition algorithm. Also the serial search will be incorporated in the simulations results, as a particular case of the hybrid search and in order to offer a benchmark for the results. The acquisition problem of any pseudorandom code (as those used in CDMA systems such as Galileo) is equivalent with the classical detection problem of testing two hypotheses  $H_0$  versus  $H_1$ :

$$\begin{cases} H_1 : \text{signal is present} \\ H_0 : \text{signal is absent} \end{cases}$$

The  $H_0$  and  $H_1$  hypotheses are in fact associated with the envelope of the correlation between the incoming signal and a locally generated reference code, with different tentative delays and Doppler frequencies. Each pair of tentative delay and Doppler frequency defines as bin (or a cell), as shown in Fig. 1. Several bins (or cells) are grouped together in a so-

called search window, as illustrated in Fig. 1. A test statistic is formed in each window, such as the maximum correlation value among all bins in a window, and that test statistic is compared with a threshold, in order to detect the presence or the absence of the signal.

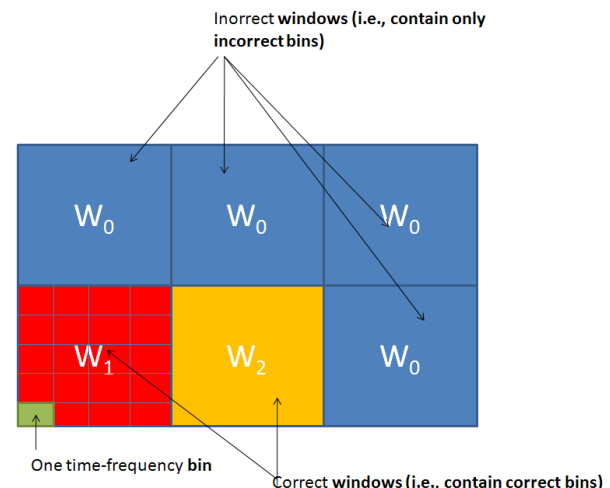


Figure 1. Illustration of hybrid search space

The classical situation, analyzed so far in the literature is the situation when the whole main correlation lobe is contained in only one window. However, due to the randomness of the channel delays, this is not always true, and it is possible to encounter a situation as shown in Fig. 2, where parts of main lobe of the correlation envelope are contained in one window, and the other parts are contained in the second window. Both windows are 'correct' windows, satisfying hypothesis  $H_1$ , and they are denoted in what follows by  $W_1$ , and  $W_2$ , as illustrated in Fig. 1. This is the case we address in this paper and that has not been reported before in literature, to the best of the author's knowledge. The benefit of studying the case of two correct search windows is that the conclusions can be used for further improving the acquisition algorithms implemented in GNSS receivers. Previous studies dealing with the mean acquisition time in GNSS signals in the presence of single correct window can be found, for example, in [1,2,3,4].

The second section of this paper presents the model of the acquisition stage that has been used for computing the mean acquisition time. Section III explains how the variable

threshold algorithm works. The results obtained from the Matlab simulations are illustrated in Section IV and the conclusions are drawn in the fifth Section.

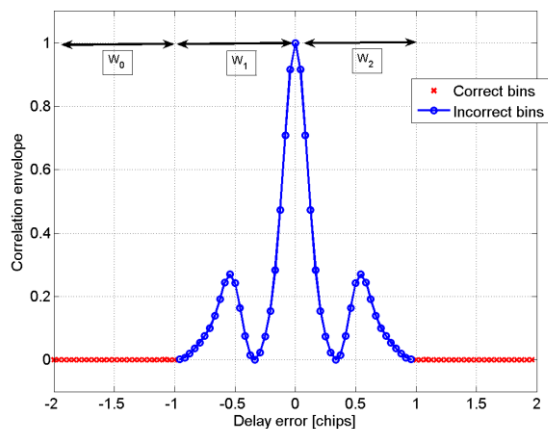


Figure 2. Example of multiple correct-window hybrid search. Galileo CBOC(-) signal, specific to E1-C, and 24.552 MHz double-sided bandwidth.

## II. ACQUISITION MODEL

From the point of positioning, only the first path (or Line of Sight, LOS) is of interest. The size of the hybrid search window typically depends on the available number of correlators. For a pure software implementation, the window length can cover the whole code uncertainty (of 1023 chips for GPS and 4092 chips for Galileo). In this situation, the hybrid search is equivalent with parallel search. However, in most of the cases, the search window length is much smaller (few tens or few hundreds of chips). We may however assume that there are at most  $Q=2$  windows containing signal cells (and thus the maximum channel delay spread is less than twice of search window length). In Fig. 1, the illustrated window length is of one chip.

Each window is formed by several cells. Their number depends on the step of scanning the time-bin hypotheses. For example, if this step is  $(\Delta t)_{bin}$  (in chips) and the window length in chips is  $L_w$ , then there are  $N$  cells per search window, where  $N$  is given by:

$$N = \frac{L_w}{(\Delta t)_{bin}} \quad (1)$$

A cell can be either a  $H_1$  (hypothesis one) cell, meaning that it contains signal coming from one channel path (the signal level is dependent on path position and on the modulation type, which defines the correlation function shape), or a  $H_0$  (hypothesis 0) cell, meaning that it contains only noise. Even in single-path case, due to the 2-chip width correlation function, we may have more than one  $H_1$  cells per window.

We denote by  $W_1$  and  $W_2$  the windows containing signal  $H_1$  cells and by  $W_0$  the windows containing only  $H_0$  cells. As explained in the previous section, the assumption with at most two windows with  $H_1$  cells is reasonable. We also assume that there are  $L_i$ ,  $i=1,2$  cells containing signal in  $W_i$  window (i.e.,  $H_1$  cells) and  $N - L_i$  cells with only noise (i.e.,  $H_0$  cells) ( $N$  being the total number of cells per window).

It is straightforward to show that, after non-coherent integration, the signal in  $H_1$  cells obeys a  $\chi^2$  non-central distribution of Cumulative Distribution Function (CDF)  $F_{nc}(\gamma, \lambda_0)$ ,  $l=1, \dots, L_i$ , and the signal in  $H_0$  cells obeys a  $\chi^2$  central distribution of CDF  $F_c(\gamma)$ . Above,  $\gamma$  is the detection threshold [5] and  $\lambda_i$  is the non-centrality parameter in cell  $L_i$ , related to signal power  $E_b$  and to the envelope of the BOC/BPSK auto-correlation function  $R(\Delta\tau_l)$  in  $l$ -th cell or bin, which is spaced with  $\Delta\tau_l$  chips from the maximum; e.g.,  $R(0) = 1$ . Thus,  $\lambda_i$  is defined as:

$$\lambda_i = E_b R(\Delta\tau_l) \quad (2)$$

For multiple dwell search ( $K$  dwells), the state transition diagram between one state to another can be divided into 3 regions, as seen in Fig. 3: transition between  $W_1$  and  $W_2$  windows, transition between  $W_2$  and  $W_0$  windows, and transitions between  $W_0$  and  $W_0$  windows. We assume that there are  $\nu$  windows in the search space: maximum 2 windows ( $W_1$  and  $W_2$ ) containing signal  $H_1$  cells (a particular case here is the situation when only the first window contains signal cells  $W_2=W_0$ ) and  $\nu - 2$  windows containing only noise  $H_0$  cells.

In here, we use also the assumption that the correct cell is at the edge between two windows ( $W_1$  and  $W_2$ ), and the acquisition state can be achieved from both  $W_1$  and  $W_2$  windows. The state flow diagram is shown in Fig. 3.  $\tau_k$  is the  $k$ -th dwell time. We used the notation  $H_M^{(k)}$  for a ‘‘missed detection’’ transfer function and the notation  $H_W^{(k)}$  for a transition from one correct window to the second correct window. We also used the notations  $H_{FA}^{(k)}$  and  $H_{NFA}^{(k)}$  for the false alarm (FA) and non-false alarm (NFA) transfer functions, at  $k$ -th dwell. The penalty factor to return from a false alarm state is denoted via  $\zeta_p$ .

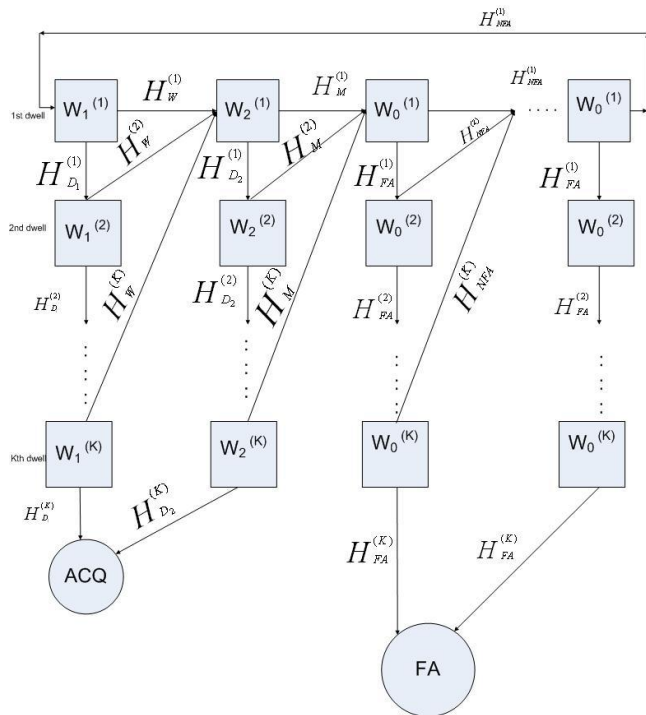


Figure 3. Flow chart for the assumed case (first path at the border between two windows).

The transfer functions shown in Fig. 3 are given by:

$$H_{D_1}^{(k)}(z) = P_{d_1}^{(k)} z^{\tau_k}, i=1,2 \quad (3)$$

$$H_W^{(k)}(z) = (1 - P_{d_1}^{(k)}) z^{\tau_k} \quad (4)$$

$$H_M^{(k)}(z) = (1 - P_{d_2}^{(k)}) z^{\tau_k} \quad (5)$$

$$H_{FA}^{(k)}(z) = P_{fa}^{(k)} z^{\tau_k} \quad (6)$$

$$H_{NFA}^{(k)}(z) = (1 - P_{fa}^{(k)}) z^{\tau_k} \quad (7)$$

and

$$H_R(z) = z^{\xi_p \tau_k} \quad (8)$$

where the detection and false alarm probabilities are:

$$P_{d_1}^{(k)} = 1 - (F_c(\gamma^{(k)}))^{N-L_1} \prod_{l=1}^{L_1} F_{nc}(\gamma^{(k)}, \bar{\lambda}_l^{(k)}) \quad (9)$$

$$P_{d_2}^{(k)} = 1 - (F_c(\gamma^{(k)}))^{N-L_2} \prod_{l=1}^{L_2} F_{nc}(\gamma^{(k)}, \bar{\lambda}_l^{(k)}) \quad (10)$$

and

$$P_{fa}^{(k)} = 1 - (F_c(\gamma^{(k)}))^N \quad (11)$$

Above,  $\gamma^{(k)}$  is the detection threshold at  $k$ -th dwell,  $k=1, \dots, K$ ,  $\lambda_l^{(k)}$  is the non-centrality parameter in  $l$ -th cell of window  $W_l$ , at  $k$ -th dwell, and is defined as:

$$\lambda_l^{(k)} = E_b R^{(k)} (\Delta \tau_l) \quad (12)$$

and  $\bar{\lambda}_l^{(k)}$  is the non-centrality parameter in  $l$ -th cell of window  $W_2$ , at  $k$ -th dwell, and is defined as:

$$\bar{\lambda}_l^{(k)} = E_b \bar{R}^{(k)} (\Delta \tau_l) \quad (13)$$

The equivalent flow chart of Fig. 3 is given in Fig. 4. The equivalent transfer functions of Fig. 4 are given below:

$$H_W(z) = H_W^{(1)}(z) + \sum_{k=1}^K H_W^{(k)}(z) \prod_{i=1}^{k-1} H_{D_1}^{(i)}(z) \quad (14)$$

$$H_M(z) = H_M^{(1)}(z) + \sum_{k=1}^K H_M^{(k)}(z) \prod_{i=1}^{k-1} H_{D_2}^{(i)}(z) \quad (15)$$

$$H_T(z) = H_{NFA}^{(1)}(z) + \sum_{k=1}^K H_{NFA}^{(k)}(z) \prod_{i=1}^{k-1} H_{FA}^{(i)}(z) \quad (16)$$

$$+ H_R(z) \prod_{i=1}^K H_{FA}^{(i)}(z)$$

From [6], the equivalent transfer function of Fig. 3 is:

$$H(z) = \sum_{i=1}^{\nu-1} p_i T_i(z) + p_\nu T(z) \quad (17)$$

where

$$T_i(z) = \frac{H_T^i(z) H_{D_1}(z)}{1 - H_W(z) H_M(z) (H_T(z))^{\nu-2}} \quad (18)$$

$$T(z) = \frac{H_{D_2}(z)}{1 - H_W(z) H_M(z) (H_T(z))^{\nu-2}} \quad (19)$$

Again, if all the states are equally probable, then:

$$p_i = \frac{1}{\nu}, i=1, \dots, \nu. \quad (20)$$

If we start from the correct state (e.g., assisted acquisition), then  $p_1 = 1$  and  $p_i = 0$ ,  $i=2, \dots, \nu$ .

The Mean Acquisition Time (MAT) can be computed as [7]:

$$MAT = \left. \frac{dH(z)}{dz} \right|_{z=1} \quad (21)$$

and it can be straightforwardly calculated numerically (e.g., via Matlab).

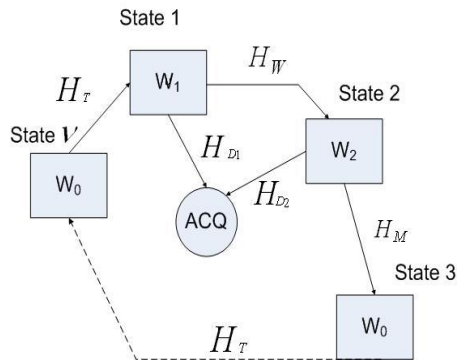


Figure 4. Equivalent flow chart for the assumed case (first path at the edge of two windows).

### III. VARIABLE THRESHOLD, FIXED DWELL TIME ALGORITHM

In order to compute the detection and false alarm probabilities needed in the MAT computation, we fixed a target false alarm at the output of all dwells (which is the product of the individual false alarm in each dwell, and will be specified in the parameters table) and we also fixed the total integration time per dwell, as the product between a certain coherent integration interval  $N_c$  and a certain non-coherent integration interval  $N_{nc}$ . With the desired false alarm and the specified coherent and non-coherent integration intervals, a variable threshold per each dwell was computed, according to eq. (11). The variable threshold was then introduced in equations (9) and (10) in order to compute the corresponding detection probabilities.

As illustrated in Fig. 5, by reducing the false alarm, we increase the detection threshold, and thus we also reduce the detection probability. It is usually preferred that the first dwell has a lower false alarm probability and a lower integration time (or dwell time), while in the sub-sequent dwells we try to improve the detection probabilities, by allowing a higher integration time and, typically, a higher false alarm probability.

### IV. SIMULATION RESULTS

The main simulation parameters, common for all considered scenarios, are illustrated in TABLE I. The number of states  $\nu$  is computed as the total number of time-Doppler bins (i.e.,  $18 \times 11691 = 210438$ ), divided by the number of bins per window (given in TABLE I). The analyzed case was the situation of a CBOC(-) modulated signal (e.g., pilot channel E1-C in Galileo, according to [8]) with a reference CBOC modulated code and a wideband receiver front-end of 24.552 MHz, as specified in [8]. Several scenarios were analyzed, as given in TABLE II. The results are presented in the following sub-sections.

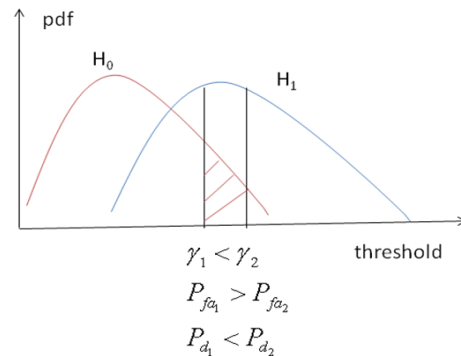


Figure 5. Illustration of the variable threshold concept.

TABLE I. PARAMETERS USED IN THE SIMULATIONS

Parameters	Value
Penalty factor $\zeta_P$	10
Time bin step $(\Delta t)_{bin}$	0.35 chips
Receiver front-end bandwidth (double-sided)	24.552 MHz
Channel type	Static, single path
Number of bins per window in the hybrid search	4000 (moderate) and 100000 (high)
Number of bins per window in the serial search	1
Galileo signal	E1-C (CBOC(-) modulation)
Doppler frequency uncertainty	From -9 kHz to +9 kHz with a step of 1 kHz (i.e., a total of 18 Doppler bins)
Code phase uncertainty	4092 chips, with a step $(\Delta t)_{bin}$ (i.e., a total of 11691 time bins)

TABLE II. DWELL PARAMETERS

	Single dwell	Two dwells	Three dwells
<i>Scenario 1</i> (global false alarm $10^{-5}$ , a global integration time of 256 ms)	$P_{fa}=[10^{-5}]$ $N_c=[16]$ $N_{nc}=[16]$	$P_{fa}=[10^{-3}$ $10^{-2}]$ $N_c=[4$ 4] $N_{nc}=[1$ 16]	$P_{fa}=[10^{-3}$ $10^{-1}$ $10^{-1}]$ $N_c=[2$ 2 4] $N_{nc}=[1$ 2 8]
<i>Scenario 2</i> (global false alarm $10^{-3}$ , a global integration time of 512 ms)	$P_{fa}=[10^{-3}]$ $N_c=[64]$ $N_{nc}=[8]$	$P_{fa}=[0.07$ 0.014] $N_c=[4$ 16] $N_{nc}=[1$ 8]	$P_{fa}=[0.2$ 0.1 0.05] $N_c=[4$ 4 4] $N_{nc}=[1$ 2 4]
<i>Scenario 3</i> (global false alarm $10^{-3}$ , a global integration time of 512 ms)	$P_{fa}=[10^{-3}]$ $N_c=[64]$ $N_{nc}=[8]$	$P_{fa}=[0.014$ 0.07 ] $N_c=[4$ 16] $N_{nc}=[1$ 8]	$P_{fa}=[0.05$ 0.1 0.2] $N_c=[4$ 4 4] $N_{nc}=[1$ 2 4]

A. Moderate number of correlators in the hybrid search

In the first analyzed situation, we assumed that each decision window has 4000 complex correlators (or bins). The results are shown in Fig. 6 to Fig. 8, for the 3 scenarios shown in TABLE II.

It is to be noticed that *Scenario 3* differs from *Scenario 2* only in that the false alarm probabilities in multi-dwell case are increasing (instead of decreasing). From the comparison of Fig. 7 with Fig. 8, we see that *Scenario 3* (increasing false alarm probabilities) gives slightly better results (than *Scenario 2*) in the 2-dwell and 3-dwell cases. As seen in the following figures, at low Carrier to Noise Ratio ( $C/N_0$ ), single-dwell approaches have very good performance (either comparable or even better than multiple-dwell approaches), in both serial and hybrid searches. At higher  $C/N_0$ , typically above 30 dB-Hz, multi-dwell approaches do bring an improvement in MAT, but the improvement from passing from 2-dwell to 3-dwell architecture is not as significant as the improvement from single dwell to 2 dwells. Also, there is a significant improvement if several correlators can be used in parallel (hybrid approach), compared to the serial case.

B. High number of correlators in the hybrid search

In the second analyzed situation, we assumed that each decision window has 100000 complex correlators (or bins), corresponding to only 2 search windows in the whole uncertainty space. The results are shown in Fig. 9 to Fig. 11. Clearly, going from 4000 to 100000 correlators per search window improves the MAT performance (the gap versus serial search is higher for higher number of correlators).

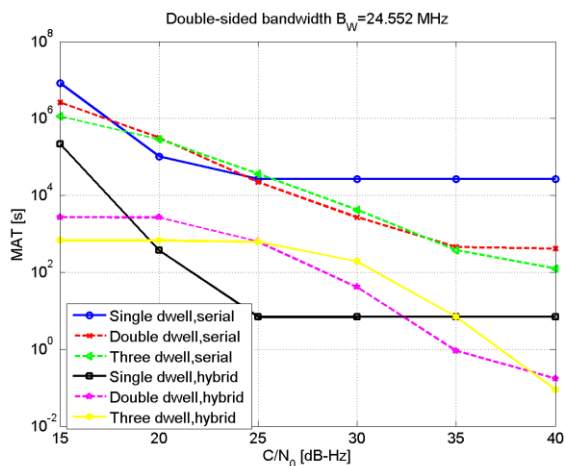


Figure 6. Performance of multi-dwell acquisition, *Scenario 1*, wideband receiver (BW=24.552 MHz), 4000 complex correlators (or number of bins per window)

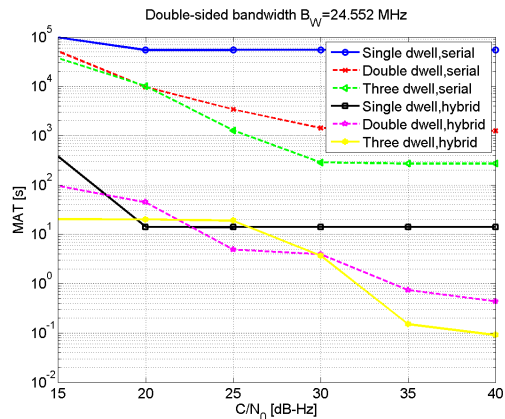


Figure 7. Performance of multi-dwell acquisition, *Scenario 2*, wideband receiver (BW=24.552 MHz), 4000 complex correlators.

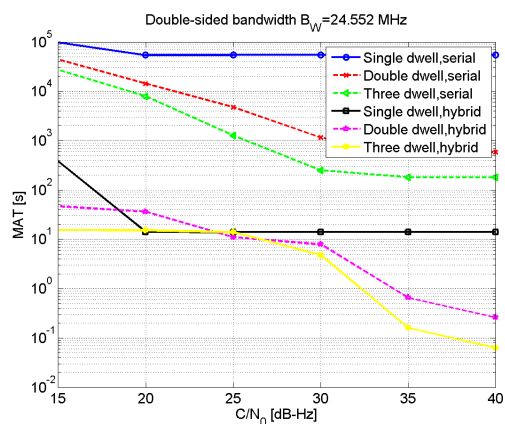


Figure 8. Performance of multi-dwell acquisition, *Scenario 3*, wideband receiver (BW=24.552 MHz), 4000 complex correlators.

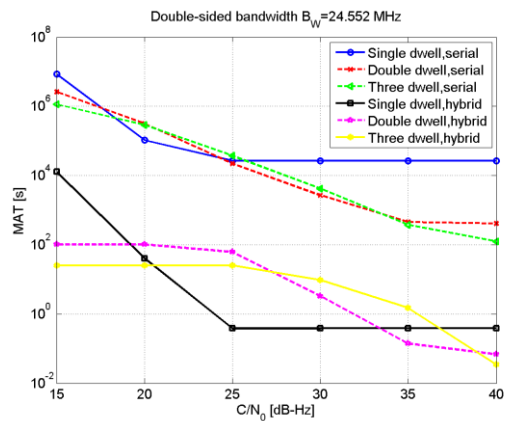


Figure 9. Performance of multi-dwell acquisition, *Scenario 1*, wideband receiver (BW=24.552 MHz), 100000 complex correlators

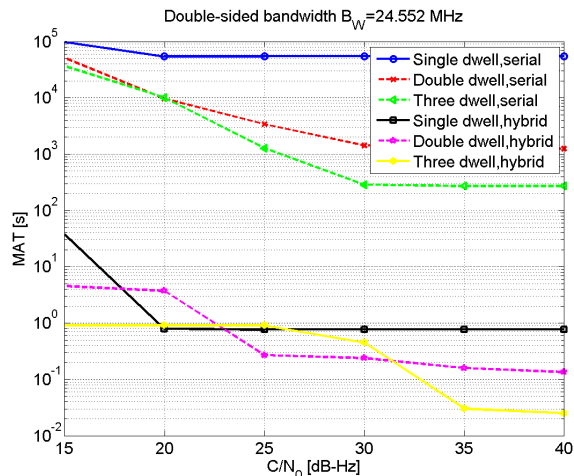


Figure 10. Performance of multi-dwell acquisition, *Scenario 2*, wideband receiver (BW=24.552 MHz), 100000 complex correlators.

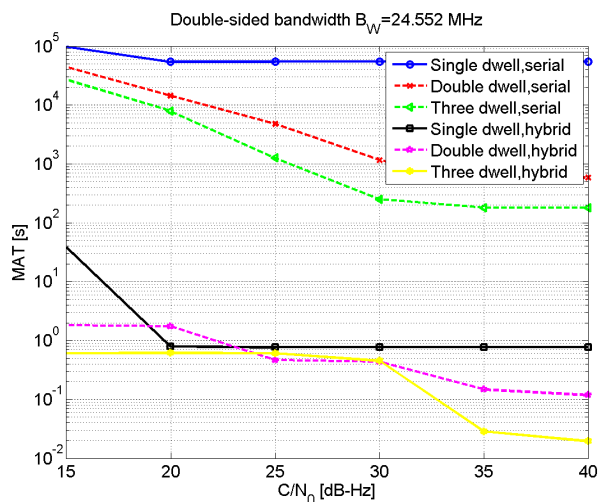


Figure 11. Performance of multi-dwell acquisition, *Scenario 3*, wideband receiver (BW=24.552 MHz), 100000 complex correlators.

## V. CONCLUSION

This paper introduces a semi-analytical expression for the computation of the Mean Acquisition Time for the hybrid search of Galileo CBOC-modulated signals, under the hypothesis of multiple correct windows (due to the randomness of the delays introduced by the wireless channel and to the width of the main correlation lobe). Simulation results under static channels and multiple correlators per search window for Galileo E1-C pilot channels were also presented. Also the serial search case was maintained as a benchmark. It was seen that increasing the number of dwells can bring some benefit in the MAT, if the parameters of each dwell (e.g., integration times and false alarm probabilities per dwell) are chosen properly. It was also seen that choosing an increasing false alarm probability per dwell (i.e., smallest false alarm at the first dwell and highest as the last dwell), in conjunction with an increasing integration time

(i.e., smallest at the first stage, highest at the last stage) offers the best results. It was also shown that increasing the coherent integration time, while keeping the same overall integration time offers slightly better MAT results. The coherent integration length is of course, limited by the presence of data bit transitions and local oscillator drifts. Further studies are dedicated to the behavior in multipath fading channels (however, analytical and semi-analytical MAT expressions for these cases are hard to get and the results are likely to be obtained in an empirical manner, via Monte-Carlo simulations).

## ACKNOWLEDGMENT

This work has been supported by the Academy of Finland and by Nokia Foundation grant. This work has also been supported partly by the Sectoral Operational Programme Human Resources Development 2007-2013 of the Romanian Ministry of Labour, Family and Social Protection through the Financial Agreement POSDRU/88/1.5/S/61178.

## REFERENCES

- [1] E. S. Lohan, A. Burian, and M. Renfors, "Acquisition of Galileo signals in hybrid double-dwell approaches", in CDROM Proceedings of ESA NAVITEC, Dec 2004.
- [2] S. Lohan, A. Lakhzouri, and M. Renfors, "Selection of the multiple-dwell hybrid-search strategy for the acquisition of Galileo signals in fading channels", in CDROM Proc. of IEEE PIMRC, Sep 2004.
- [3] A. Lakhzouri, E. S. Lohan, and M. Renfors, "Hybrid-search single and double-dwell acquisition architectures for Galileo signal", in CDROM Proc. of IST mobile & wireless communications workshop, Jun 2004.
- [4] A. Konovaltsev, A. Hornbostel, H. Denks, and B. Bandemer, "Acquisition Trade-Offs for Galileo SW Receiver". In: European Navigation Conference ENC-GNSS 2006, ENC2006 CD. European Navigation Conference and Exhibition 2006, 2006-05-07 - 2006-05-10, Manchester, UK.
- [5] S. Turunen, "Network assistance: what will new GNSS signals bring to it," in *Inside GNSS*, Spring 2007, pp. 35–41.
- [6] B.J. Kang and I.K. Lee, "A performance comparison of code acquisition techniques in DS-CDMA system", *Wireless Personal Communications*, vol. 25, 2003, pp. 163-176.
- [7] A. Polydoros and C.L. Weber, "A unified approach to serial search spread-spectrum code acquisition – Parts I and II: A matched filter receiver", *IEEE Trans. On Comm.*, vol 32(5), May 1984, pp. 542-560.
- [8] European Commission/GSA, "Galileo Signal In Space- Interface Control Documentation" (Galileo SIS-ICD), version Feb 2010.